AAC
Journals.ASM.org

Ceftaroline Increases Membrane Binding and Enhances the Activity of Daptomycin against Daptomycin-Nonsusceptible Vancomycin-Intermediate *Staphylococcus aureus* in a Pharmacokinetic/Pharmacodynamic Model

Brian J. Werth,[a] George Sakoulas,[c,d] Warren E. Rose,[f] Joseph Pogliano,[e] Ryan Tewhey,[g] Michael J. Rybak[a,b]

Anti-Infective Research Laboratory, Department of Pharmacy Practice, Eugene Applebaum College of Pharmacy and Health Sciences,[a] and Department of Internal Medicine, Division of Infectious Diseases, School of Medicine,[b] Wayne State University, Detroit, Michigan, USA; Department of Medicine, New York Medical College, Valhalla, New York, USA[c]; University of California San Diego School of Medicine, La Jolla, California, USA[d]; University of California San Diego Division of Biology, La Jolla, California, USA[e]; School of Pharmacy, University of Wisconsin—Madison, Madison, Wisconsin, USA[f]; and Scripps Translational Science Institute, Scripps Research Institute, La Jolla, California, USA[g]

New antimicrobial agents and novel combination therapies are needed to treat serious infections caused by methicillin-resistant *Staphylococcus aureus* (MRSA) with reduced susceptibility to daptomycin and vancomycin. The purpose of this study was to evaluate the combination of ceftaroline plus daptomycin or vancomycin in an *in vitro* pharmacokinetic/pharmacodynamic model. Simulations of ceftaroline-fosamil at 600 mg per kg of body weight every 8 h (q8h) (maximum free-drug concentration in serum [fC_{max}], 15.2 mg/liter; half-life [$t_{1/2}$], 2.3 h), daptomycin at 10 mg/kg/day (fC_{max}, 11.3 mg/liter; $t_{1/2}$, 8 h), vancomycin at 2 g q12h (fC_{max}, 30 mg/liter; $t_{1/2}$, 6 h), ceftaroline plus daptomycin, and ceftaroline plus vancomycin were evaluated against a clinical, isogenic MRSA strain pair: D592 (daptomycin susceptible and heterogeneous vancomycin intermediate) and D712 (daptomycin nonsusceptible and vancomycin intermediate) in a one-compartment *in vitro* pharmacokinetic/pharmacodynamic model over 96 h. Therapeutic enhancement of combinations was defined as ≥2 $\log_{10}$ CFU/ml reduction over the most active single agent. The effect of ceftaroline on the membrane charge, cell wall thickness, susceptibility to killing by the human cathelicidin LL37, and daptomycin binding were evaluated. Therapeutic enhancement was observed with daptomycin plus ceftaroline in both strains and vancomycin plus ceftaroline against D592. Ceftaroline exposure enhanced daptomycin-induced depolarization (81.7% versus 72.3%; $P = 0.03$) and killing by cathelicidin LL37 ($P < 0.01$) and reduced cell wall thickness ($P < 0.001$). Fluorescence-labeled daptomycin was bound over 7-fold more in ceftaroline-exposed cells. Whole-genome sequencing and mutation analysis of these strains indicated that change in daptomycin susceptibility is related to an *fmtC* (*mprF*) mutation. The combination of daptomycin plus ceftaroline appears to be potent, with rapid and sustained bactericidal activity against both daptomycin-susceptible and -nonsusceptible strains of MRSA.

Infections caused by methicillin-resistant *Staphylococcus aureus* (MRSA) with reduced susceptibility to vancomycin (VAN) and daptomycin (DAP) are often associated with high bacterial density; failure of prior antimicrobial therapies, including VAN; and poor clinical outcomes (1, 2). Alternative agents currently recommended are limited by side effects, suboptimal plasma concentrations, and bacteriostatic activity, which may not be suitable for managing serious, high-inoculum infections, such as infective endocarditis (1, 3). Consequently, new antimicrobials and novel combinations must be explored in order to establish safer and more effective alternatives for managing infections caused by MRSA with reduced susceptibility to DAP and VAN.

Ceftaroline-fosamil (CPT-F) is a broad-spectrum cephalosporin approved by the FDA for the management of community-acquired bacterial pneumonia and acute bacterial skin and skin structure infections. CPT, the active metabolite of CPT-F, has activity against MRSA, heterogeneous VAN-intermediate *S. aureus* (hVISA), VISA, VAN-resistant *S. aureus* (VRSA), and DAP-nonsusceptible (DNS) *S. aureus* (4). This activity is conferred by ceftaroline's affinity for multiple penicillin binding protein (PBP) subtypes, including PBP2a, which mediates oxacillin (OXA) resistance (4). While CPT is reliably bactericidal against most strains of *S. aureus*, some *in vitro* data indicate that it may be more active against hVISA and VISA strains than strains that are fully susceptible to VAN (5, 6). The phenomenon referred to as the "seesaw" effect, whereby susceptibility to antistaphylococcal beta-lactams (ASBLs) increases as glyco- and lipopeptide susceptibility decreases, may explain the enhanced CPT activity that has been observed (7–9). A possible explanation for this effect might be related to differential PBP expression induced by glycopeptide exposure in VISA strains (10–13).

DAP is rapidly bactericidal against *S. aureus*, including VISA and hVISA strains, and has been shown to be synergistic with OXA and other ASBLs against DNS MRSA (14). Exposure to beta-lactams increases binding of DAP and cationic microbicidal peptides to cell membranes and enhances the bactericidal activity of these compounds in both MRSA and enterococci (14, 15). CPT appears

Received 1 August 2012 **Returned for modification** 3 September 2012
Accepted 6 October 2012
Published ahead of print 15 October 2012
Address correspondence to Michael J. Rybak, m.rybak@wayne.edu.

doi:10.1128/AAC.01586-12

to be substantially more effective than high-dose DAP (10 mg/kg of body weight/day) against VISA and hVISA strains when the DAP MIC is ≥2 mg/liter (5). Based on the synergy observed between DAP and OXA and the superior activity of CPT against DNS *S. aureus*, CPT plus DAP has the potential to be a powerful combination. The objectives of the present study were to evaluate the combination of CPT plus DAP for evidence of therapeutic enhancement in a preliminary one-compartment pharmacokinetic/pharmacodynamic (PK/PD) model simulating a high-inoculum infection with DAP- and VAN-susceptible and -nonsusceptible MRSA and to examine the mechanism for this interaction if one was found.

MATERIALS AND METHODS

Bacterial strains. One clinical isogenic strain pair isolated from a patient with prolonged bacteremia secondary to osteomyelitis was evaluated. The parent strain (D592) is a DAP-susceptible (DS) hVISA strain that mutated into a DNS VISA strain (D712) over a 20-day period of antimicrobial therapy that included VAN and DAP (14).

Antimicrobials. DAP and VAN were purchased commercially from Cubist Pharmaceuticals (Lexington, MA) and Sigma Chemical Co. (St. Louis, MO), respectively. CPT was provided by Forest Laboratories, Inc. (New York, NY). Bodipy-fluorescein-labeled daptomycin was provided by Cubist Pharmaceuticals (Lexington, MA).

Media. Cation-adjusted Mueller-Hinton broth (CAMHB) (Difco, Detroit, MI), containing 25 mg/liter calcium and 12.5 mg/liter magnesium, was used for PK/PD models with VAN and CPT. Due to the calcium-dependent mechanism of DAP, MHB supplemented with 50 mg/liter calcium and 12.5 mg/liter magnesium was used for models utilizing DAP. Colony counts were determined using tryptic soy agar (TSA) (Difco, Detroit, MI) plates.

Susceptibility testing. MICs of study antimicrobial agents were determined in duplicate by broth microdilution at 10^6 CFU/ml according to CLSI guidelines. All samples were incubated at 37°C for 18 to 24 h (16). Glycopeptide heteroresistance in D592 was confirmed by previously described methods (30).

***In vitro* PK/PD model.** An *in vitro* one-compartment PK/PD model with a 250-ml capacity and input and outflow ports was used. The apparatus was prefilled with medium, and antimicrobials were administered as boluses over a 96-hour time period. Prior to each experiment, bacterial lawns from an overnight growth on TSA were suspended and added to each model to obtain a starting inoculum of ~10^8 CFU/ml. Fresh medium was continuously supplied and removed from the compartment along with the drug via a peristaltic pump (Masterflex; Cole-Parmer Instrument Company, Chicago, IL) at an appropriate rate to simulate the average human half-lives of the antimicrobials. The antimicrobial regimens evaluated were simulations of CPT-F at 600 mg every 8 h (q8h) (maximum free-drug concentration in serum [fC_{max}], 15.2 mg/liter; half-life [$t_{1/2}$], 2.3 h; protein binding, 20%) (17), DAP simulations of 10 mg/kg q24h (fC_{max}, 11.3 mg/liter; $t_{1/2}$, 8 h; protein binding, 92%) (18), VAN simulations of 2 g q12h (fC_{max}, 30 mg/liter; $t_{1/2}$, 6 h; protein binding, ~55%) (19), CPT-F at 600 mg q8h plus DAP at 10 mg/kg q24h, and CPT-F at 600 mg q8h plus VAN at 2 g q12h. The models were performed in duplicate to ensure reproducibility. Supplemental DAP and VAN were added at an appropriate rate to CPT combination models to compensate for the higher flow rate required to simulate CPT clearance (20).

Pharmacodynamic analysis. Samples from each model were collected at 0, 4, 8, 24, 28, 32, 48, 56, 72, and 96 h in duplicate and diluted in cold 0.9% saline. Colony counts were determined by spiral plating appropriate dilutions using an automatic spiral plater (WASP; DW Scientific, West Yorkshire, England) to enumerate CFU/ml and avoid antibiotic carryover. Colonies were counted using a laser colony counter (ProtoCOL; Synoptics Ltd., Frederick, MD). If the anticipated dilution was near the MIC, vacuum filtration was used to avoid antibiotic carryover. When vacuum filtration was used, samples were washed through a 0.45-μm filter with normal saline to remove the antimicrobial agent. For both methods, plates were incubated at 37°C for 24 h before colonies were counted. These methods have a lower limit of reliable detection of 1 $\log_{10}$ CFU/ml. The total reduction in $\log_{10}$ CFU/ml over 96 h was determined by plotting model time-kill curves based on the number of remaining organisms over the 96-h time period. Bactericidal activity (99.9% kill) was defined as a ≥3-$\log_{10}$-CFU/ml decrease in colony count from the initial inoculum. Bacteriostatic activity was defined as a <3-$\log_{10}$-CFU/ml reduction in colony count from the initial inoculum, and inactivity was defined as no observed reduction in initial inocula. The time to achieve a 99.9% bacterial load reduction was determined by linear regression or by visual inspection (if r^2 was ≤0.95). Therapeutic enhancement of combinations was defined as ≥2-$\log_{10}$-CFU/ml reduction over the most active single agent.

Pharmacokinetic analysis. Pharmacokinetic samples were obtained through the injection port of each model at 0, 1, 2, 4, 8, 24, 32, 48, 56, 72, and 96 h for verification of target antibiotic concentrations. All samples were stored at −70°C until ready for analysis. CPT concentrations were determined by bioassay using *Bacillus subtilis* ATCC 6633. Blank 1/4-in disks were spotted with 10 μl of standard concentrations or samples. Each standard was tested in duplicate by placing the disk on agar plates (antibiotic medium number 11) inoculated with a 0.5 McFarland suspension of the test organism. This assay demonstrated an intraday coefficient of variance of less than 10% for 2.5-, 10-, and 40-mg/liter standards. For DAP, 1/4-in holes were punched in antibiotic medium number 5 agar plates inoculated with *Micrococcus luteus* (ATCC 9341) and filled with 50 μl of the standards or samples. This assay was found to have an intraday coefficient of variance of less than 11% for 2.5-, 7.5-, and 15-mg/liter standards. Each standard and sample was tested in duplicate. The plates were incubated for 18 to 24 h at 37°C, at which time the zone sizes were measured using a protocol reader (Protocol; Microbiology International, Frederick, MD). Concentrations of VAN were determined using a fluorescence polarization immunoassay (TDX assay; Abbott Diagnostics). The VAN assay has a limit of detection of 2.0 mg/liter with an interday coefficient of variance of less than 12% for low, medium, and high standards. The half-lives, areas under the curve (AUC), and peak concentrations of the antibiotics were determined by the trapezoidal method, utilizing PK Analyst software (version 1.10; MicroMath Scientific Software, Salt Lake City, UT).

Resistance. Emergence of resistance was evaluated at 96 h by plating 100-μl samples from the model on Mueller-Hinton agar (MHA) or brain heart infusion agar (BHIA) plates supplemented with DAP, CPT, or VAN at a concentration 3 times the MIC of the tested antibiotic. The plates were examined for growth after 24 and 48 h of incubation at 35 to 37°C. Resistant colonies growing on screening plates were evaluated by the Etest or broth microdilution method to determine the MIC. If resistance was detected at the end of the model, additional screening was performed to identify the first occurrence of resistance.

Membrane surface charge. The relative membrane charge was evaluated by a previously described cytochrome *c* binding methodology with modifications (21). Cells grown overnight in 25 ml of brain heart infusion broth (BHIB) containing 0.25 times the MIC of CPT or plain BHIB were pelleted, washed twice with MOPS (morpholinepropanesulfonic acid) buffer (20 mM; pH 7.0), and then resuspended in MOPS buffer and adjusted to an optical density at 600 nm (OD_{600}) of 4. Cytochrome *c* was dissolved in MOPS (10 mg/ml), and then 0.1 ml was added to 0.9 ml of bacterial suspension. After 30 min of incubation at 21°C with gentle shaking, the cells were centrifuged, and the cytochrome *c* remaining in the supernatant was quantitated by comparing the OD_{530} of samples with that of a standard curve. Assays were performed in triplicate, and the results were expressed as means and standard deviations (SD).

Cathelicidin LL37 microbicidal assay. Both strains were grown to stationary phase (16 to 20 h) in lysogeny broth (LB) in either the presence or absence of 0.1 mg/liter of CPT, pelleted, washed with PBS, and exposed

at an inoculum of 10^5 CFU/ml to 128 μM LL-37 in RPMI-5% LB. The percentage of surviving bacteria (±SD) after 1.5 h and 3 h of incubation at 37°C was calculated by plating on blood agar plates.

Membrane potential assay. DAP membrane depolarization was evaluated as previously described (22). Briefly, strains D592 and D712 were grown to stationary phase overnight in 5 ml of BHIB in the presence and absence of CPT at a concentration 0.25 times the MIC. After overnight growth, 1 ml of this suspension was used to inoculate 25 ml of Mueller-Hinton broth (MHB), and the cells were grown to early exponential phase, pelleted, washed twice with HEPES buffer (pH 7.2, containing 50 mg/liter Ca^{2+}), and then resuspended in HEPES (OD_{600} = 0.2). Aliquots were transferred to a cuvette containing a stir bar, and then KCl (100 mM) was added and the cuvette was placed in the heated chamber of a Fluoro-Max-3 spectrofluorometer (λ excitation = 622 nm and λ emission = 670 nm at 37°C) (Horiba Jobin Yvon Inc., Edison, NJ). The cells were incubated with the membrane potential-sensitive dye DiSC3 (16) (0.1 mg/ml) for 10 min. The conditions included CPT-exposed cells plus DAP (8 mg/liter), unexposed cells plus DAP (8 mg/liter), nisin (25 mg/liter) as a positive control, and unexposed cells without nisin or DAP as a negative control. The membrane-depolarizing activity of DAP over 60 min was calculated as follows: percent depolarization = [(Fd or Fde − Fc)/(Fn − Fc)] × 100, where Fd, Fde, Fc, and Fn are fluorescence measurements with DAP, DAP in CPT-exposed cells, no antibiotic, and nisin, respectively.

Binding of fluorescent daptomycin. Bacteria were grown to an OD_{600} of 0.6, grown for an additional 1 h with or without CPT at 1 mg/liter, and then incubated with 16 μg/ml daptomycin–boron-dipyrromethene (bodipy) for 10 min, washed three times in medium to remove unincorporated label, stained with 1 μg/ml DAPI (4′,6-diamidino-2-phenylindole), and placed on a 1% agarose pad for imaging in an Applied Precision deconvolution fluorescence microscope as described previously (23). For quantitation of daptomycin-bodipy fluorescence, images from each sample were collected using identical camera exposures. Image J was used to measure the average fluorescence intensity of individual pixels for 150 untreated cells and 200 ceftaroline-treated cells. The average fluorescence intensity of individual pixels for the background was also measured and subtracted from the cells to generate an accurate measurement of daptomycin-bodipy binding.

Whole-genome sequencing and mutation analysis. Whole-genome sequencing was performed on both D592 and D712 on a multiplexed lane of an Illumina HiSeq 2000. Briefly, DNA from stationary-phase cultures was extracted using a Biostic DNA isolation kit (MO BIO Laboratories, Carlsbad, CA). Three micrograms of DNA was sheared to an average size of 300 bp by adaptive-force acoustics using a Covaris S2 (Covaris, Woburn, MA), and standard library preparation was performed with full-length adapters and barcodes using the NEBNext master mix set (New England BioLabs, Ipswich, MA). Samples were enriched for 5 cycles and size selected at around 400 bp prior to sequencing. Approximately 4 million 100-bp paired-end reads were acquired per sample using Illumina's v3 chemistry. Samples were mapped to the MRSA Mu50 reference genome with the aligner Stampy utilizing the BWA flag (24–26). Reads underwent realignment and base quality recalibration prior to variant calling with GATK (27). Variations relative to Mu50 that were present in only one of the two isolates were identified and functionally annotated using a combination of custom Perl scripts. In addition to mapping the reads to Mu50, *de novo* contigs were also built with the overlap assembler EDENA v3 (28). Reads from D712 were mapped using the same procedure as with Mu50 but using the *de novo* contigs of D592 as the reference. We also performed cross comparisons of the D592 and D712 contigs to look for large structural differences. In both cases, the variation identified had perfect agreement with the Mu50 reference mapping.

TEM. Single models of D712 against simulated regimens of DAP, CPT, and DAP plus CPT described above were run for 18 h. After 18 h of drug exposure, 30- to 120-ml samples were collected and centrifuged to collect a sufficient sample of bacteria for imaging. Cell wall thickness (CWT) was determined by Transmission electron microscopy (TEM) as described previously (29). Ultrathin sections were evaluated at a magnification of ×48,000 with a JEOL 100CX electron microscope, and images were captured with a MegaView III side-mounted digital camera. The resulting images were analyzed using ImageJ 1.39t software. CWT was determined for at least 15 cells per sample using four separate quadrants of each cell for a total of ≥100 measurements per sample.

Statistical analysis. Changes in numbers of CFU/ml at 24, 48, 56, 72, and 96 h were compared by analysis of variance with Tukey's post hoc test. Cytochrome *c* binding and depolarization results were compared using Student *t* tests. A *P* value of ≤0.05 was considered significant. All statistical analyses were performed using SPSS Statistical Software (release 20.0; SPSS, Inc., Chicago, IL).

RESULTS

Susceptibility testing. D712 MICs were 0.5, 4, and 4 mg/liter, and D592 MICs were 1, 0.5, and 2 mg/liter for CPT, DAP, and VAN, respectively. A VAN population analysis profile (PAP) of D592 revealed an AUC/AUC ratio of 1.0367 to Mu3, indicating heteroresistance to glycopeptides.

***In vitro* PK/PD model.** The observed PK parameters were within 1%, 9%, and 18% of target values for DAP, CPT, and VAN, respectively. For CPT, the average observed fC_{max} was 15.76 ± 1.23 mg/liter (target, 15.2 mg/liter; protein binding, 20%), with an average $t_{1/2}$ of 2.10 ± 0.193 h (target, 2.3 h). The time above the MIC ($T >$ MIC) was 100% of the 8-hour dosing interval for both strains, with an average minimum free-drug concentration (fC_{min}) of 1.14 mg/liter. For DAP, the average observed fC_{max} was 11.28 mg/liter ± 0.765 mg/liter (target, 11.2 mg/liter; protein binding, 92%), with an average $t_{1/2}$ of 7.99 ± 0.056 h (target, 8 h), and the average free trapezoidal AUC from 0 to 24 h (AUC_{0-24}) was 120.9 ± 2.7 mg · h/ml. For VAN, the average fC_{max} was 27.96 ± 0.149 mg/liter (target, 30 mg/liter; protein binding, 50 to 55%), with an average $t_{1/2}$ of 4.99 h ± 0.028 h (target, 6 h) and an average free-drug AUC from 0 to 24 h ($fAUC_{0-24}$) of 336.9 ± 1.3 mg · h/ml.

Against D712 (Fig. 1A) DAP and VAN monotherapy demonstrated minimal bacteriostatic activity. CPT monotherapy demonstrated sustained bactericidal activity. The addition of CPT to DAP demonstrated therapeutic enhancement against the strain, resulting in bactericidal activity by 8 h and significantly better killing than any other therapy at all time points after 28 h ($P <$ 0.01). The combination of CPT plus VAN resulted in significantly greater reduction in $\log_{10}$ CFU/ml over all regimens, except for CPT plus DAP at 96 h, but did not meet criteria for therapeutic enhancement. A similar relationship was observed with the parent strain, D592 (Fig. 1B). Treatment with DAP plus CPT and VAN plus CPT resulted in therapeutic enhancement and significantly greater reduction in $\log_{10}$ CFU/ml than all other regimens at 96 h (Table 1). DAP plus CPT was not significantly more active than VAN plus CPT in this strain; however, it did result in bactericidal activity more rapidly than any other regimen (5.46 h versus 15.62 h). DAP, VAN, and CPT monotherapies were bacteriostatic against D592 at 96 h. No resistant mutants were recovered from any of the models with either organism by 96 h.

Membrane surface charge, depolarization, and cathelicidin LL37 microbicidal assays. Assessment of surface charge by cytochrome *c* binding showed no detectable difference in surface charge. In LL37 killing assays, DAP-NS strain D712 showed considerably reduced killing compared to DAP-susceptible D592. Killing by human cathelicidin LL37 was significantly enhanced at 1.5 and 3 h by preexposure of both strains to subinhibitory concentrations (0.1 mg/liter) of CPT ($P <$ 0.01) (Fig. 2). DAP-in-

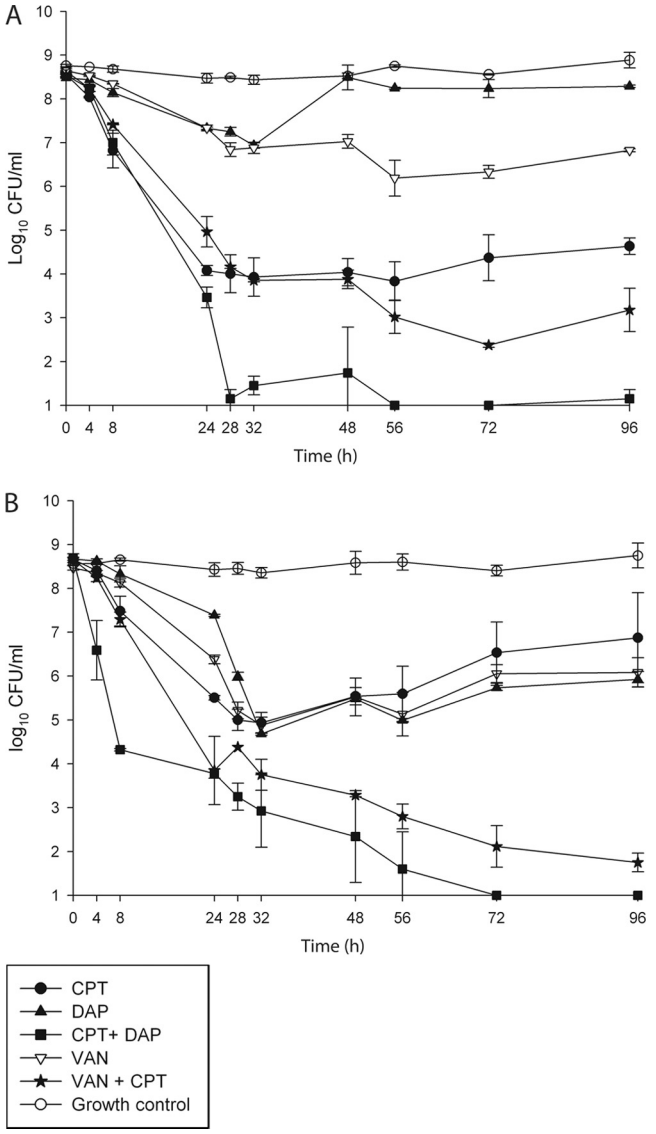

FIG 1 Activity of CPT, DAP, and VAN alone and in combination against D712 (A) and D592 (B). The error bars indicate SD.

duced membrane depolarization was enhanced in the presence of CPT (81.7% versus 72.3%; $P = 0.03$).

Binding of fluorescent daptomycin. We measured the ability of a fluorescent derivative of daptomycin to interact with the

TABLE 1 *In vitro* activity of regimens tested against D712 and D592 after 96 h

Regimen	Log_{10} CFU/ml at 96 h	
	D712	D592
DAP	8.29 ± 0.03[a]	5.92 ± 0.18[a]
VAN	6.82 ± 0.04[a]	6.08 ± 0.33[a]
CPT	4.63 ± 0.19[a]	6.87 ± 1.15[a]
DAP + CPT	1.15 ± 0.20[b]	1.00 ± 0.00[b]
VAN + CPT	3.18 ± 0.49[a]	1.75 ± 0.21[b]

[a] Significantly different than DAP plus CPT ($P \leq 0.001$).
[b] Therapeutic enhancement.

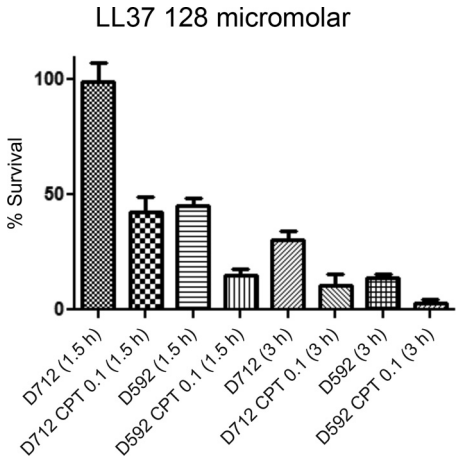

FIG 2 Percent survival of D712 and D592 at 1.5 and 3 h with 128 μM LL37 in the presence and absence of subinhibitory concentrations (0.1 mg/liter) of CPT. The error bars indicate SD.

membranes of D712. Daptomycin-bodipy showed almost no binding to the membranes of untreated cells (Fig. 3A) but bound strongly when cells were preincubated with 1 μg/ml ceftaroline for 1 h (Fig. 3B). Quantitation of fluorescence intensity showed that binding increased dramatically (>7-fold) from an average of 9 counts per pixel for untreated cells ($n = 150$ cells) compared to an average of 70 counts per pixel ($n = 200$ cells) for ceftaroline-treated cells.

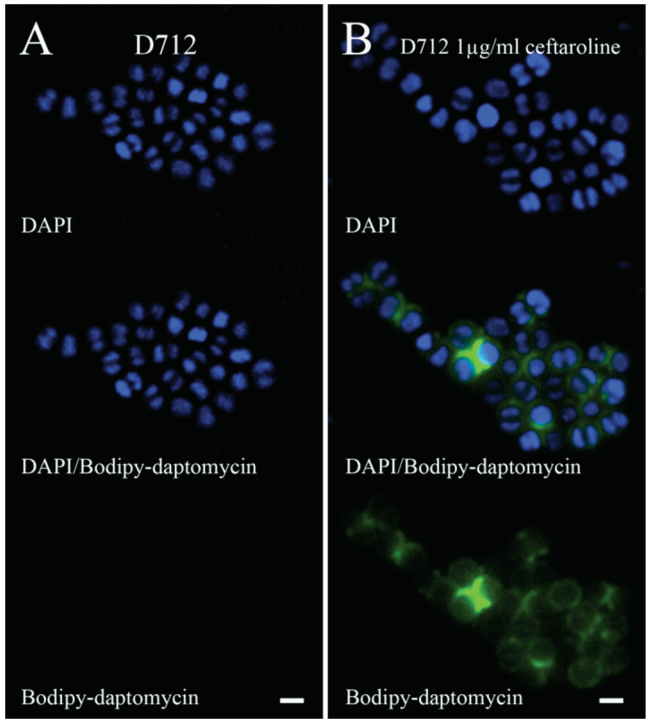

FIG 3 Binding of fluorescent daptomycin to D712 increased dramatically when cells were preincubated with ceftaroline. (A) In cells not treated with ceftaroline, daptomycin-bodipy failed to show significant binding to the membrane. (B) Daptomycin-bodipy intensely stained the membranes of cells pretreated for 1 h with 1 μg/ml ceftaroline. Scale bars, 1 μm. The tiffs used to construct the figure were adjusted identically for each sample.

TABLE 2 Mutational differences between daptomycin-susceptible hVISA D592 and daptomycin nonsusceptible VISA D712

Position based on MRSA Mu50 genome	D592→D712		
	Base pair	Amino acid	Gene
1440962	T→C	L→S nonsynonymous	SAV1360 *fmtC* (*mprF*)
1608916	A→G	I→I synonymous	SAV1491 respiratory response protein
1960627	G→A	Noncoding	NA[b]
2448257[a]	C→A	D→E nonsynonymous	SAV2324 transcriptional regulator
2592882	G→A	A→V nonsynonymous	SAV2455 endo-1,4-beta-glucanase

[a] Reference strain Mu50 has an A at position 2448257, not a C, indicating a mutation in D592.
[b] NA, not applicable.

Full-genome sequencing and mutation analysis. Full-genome sequencing revealed 5 single-nucleotide variants (SNVs) between D592 and D712 (Table 2). Three of these SNVs resulted in nonsynonymous amino acid substitutions, and 1 resulted in a change in the *fmtC* (*mprF*) gene, which is known to be associated with the development of nonsusceptibility to daptomycin and host cationic microbicidal peptides (31).

Transmission electron microscopy. Due to the enhanced activity observed with CPT and CPT in combination with DAP against D712, this strain was selected for evaluation of drug-induced changes in CWT by TEM (Fig. 4 and 5A, B, C, and D). At baseline, the average CWT was 31.56 nm. CPT exposure resulted in an average reduction in CWT of 8.94 nm ($P < 0.001$), DAP-plus-CPT exposure increased the CWT by an average of 2.42 nm ($P = 0.02$), and DAP alone resulted in a nonsignificant increase (1.28 nm) in CWT compared to unexposed cells.

DISCUSSION

Although infections with DNS MRSA are not common, they are associated with serious, deep-seated infections that require long treatment duration and have high rates of failure with typical antimicrobial regimens (1, 2). The optimal therapeutic regimen for the treatment of complicated or refractory bacteremia with MRSA with reduced susceptibility to VAN and DAP is unknown. The MRSA consensus guidelines suggest that combination therapy should be considered in this setting, but it is unclear which combination of drugs is most appropriate (3). *In vitro* and limited clinical data suggest that daptomycin in combination with trimethoprim-sulfamethoxazole (TMP-SMX) or an antistaphylococcal beta-lactam may be suitable options for refractory bacteremia with DNS MRSA (3, 14, 32–34). In this study, we have demonstrated that the combination of DAP and CPT has rapid and sustained bactericidal activity against DS, as well as DNS, strains. This combination may be more appealing to clinicians, who may not feel comfortable using DAP in combination with classic ASBLs against DNS MRSA, as neither agent is technically susceptible. Another potential advantage of this combination over combinations with classic ASBLs is that the rapid and complete reduction of the high bacterial inoculum observed may allow eventual de-escalation to CPT monotherapy, as has been successful *in vitro* with the combination of DAP plus TMP-SMX (35). Therapeutic de-escalation is especially appealing for conditions like infective endocarditis and osteomyelitis, where DNS and VISA strains are more likely and treatment duration is weeks to months. De-escalation to CPT in this setting may be pharmacoeconomically advantageous, as well. Further research is warranted to determine the optimal duration of CPT-plus-DAP therapy and the optimal timing and antimicrobial selections involved in therapeutic de-escalation.

The enhanced activity observed in the model with the combination of DAP plus CPT seems to be mediated through enhanced binding of the DAP-calcium complex secondary to increased membrane negativity, as evidenced by increased activity of LL37, binding of bodipy DAP, and enhanced membrane depolarization in CPT-exposed cells. This proposed mechanism of therapeutic enhancement is consistent with what has been published regarding the combination of DAP and beta-lactams in both staphylococci and enterococci (9, 14, 15). Although significant changes in cytochrome *c* binding in CPT-exposed cells were not observed in this study, the assay may not have been sensitive enough to detect the difference in membrane charge caused by subinhibitory concentrations of CPT, as these concentrations are much lower than those used in similar studies with other beta-lactams to which the organism is resistant (14, 15, 33).

In this experiment, we also observed improved activity of VAN when combined with CPT against both strains; however, this enhancement was greatest against the DS hVISA strain (D592). Other investigators have documented enhanced activity against MRSA, including hVISA, with the addition of traditional ASBLs to vancomycin in similar *in vitro* models (36, 37). Additional studies are warranted to further explore the combination of VAN plus CPT in other strains. A possible mechanism for this synergistic interaction may be related to the cell wall-thinning effects observed in CPT-exposed cells. MRSA with reduced susceptibility to VAN, such as VISA, are known to have thick cell walls due to an overproduction of loosely cross-linked peptidoglycan that sequesters vancomycin on the surface of the cell, preventing adequate binding to critical internal cell wall structures (11). The reduction in CWT after CPT exposure may allow VAN to penetrate into the septum, which would otherwise be protected by the thick layers of peptidoglycan, and may account for the increased activity observed with this combination.

Cell wall thickening has been associated with increases in VAN and DAP MICs, so it is unclear why DAP-plus-CPT-exposed cells developed thicker cell walls. An *in vitro* evaluation of DAP in combination with OXA noted that this regimen prevented the emergence of DAP resistance with prolonged exposure but resulted in significantly thicker cell walls than DAP alone (38). This effect of

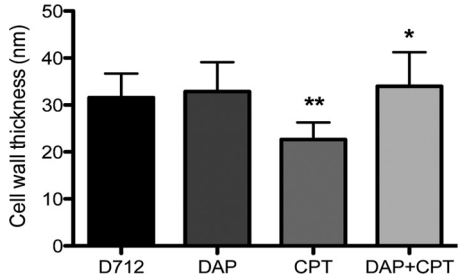

FIG 4 Cell wall thickness; comparisons relative to baseline (D712). **, $P < 0.001$; *, $P = 0.02$.

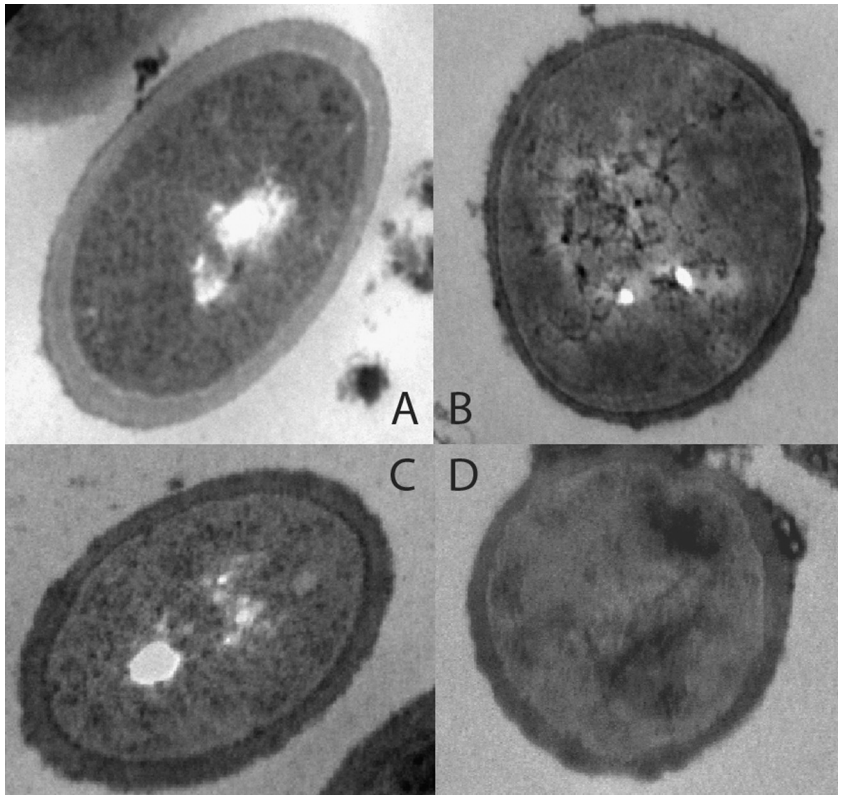

FIG 5 (A) D712 without drug exposure. (B) D712 with CPT exposure. (C) D712 with DAP exposure. (D) D712 with DAP-plus-CPT exposure.

thickened cell walls but enhanced DAP susceptibility in the presence of antistaphylococcal beta-lactam antibiotics is similar to our current findings with CPT. However, recent studies have found that DAP nonsusceptibility is not always linked to cell wall thickness but may be related to other physiologic changes in the cell envelope (39). Cell membrane fluidity, one of the identified changes in DAP-resistant strains, is reduced in response to cell wall-degrading compounds (40). It is of further interest that if cell membrane fluidity is altered in the presence of CPT, it may lead to the enhanced binding and activity of DAP identified in this study. These findings, along with prior reports of increased CWT after exposure to beta lactams, DAP, or DAP plus beta-lactam, suggest that CWT *per se* may not be functionally relevant in mediating reduced susceptibility to DAP in VISA (32). Additional research is warranted to determine the relevance of cell wall thickening in the setting of this combination.

A potential limitation of this study is related to the lack of bactericidal activity of DAP against the susceptible strain D592. This experiment was repeated in duplicate multiple times to confirm these results. The strain consistently showed a delayed response to DAP and regrew after 32 h but did not develop nonsusceptibility. In similar *in vitro* models, DAP consistently demonstrates rapid bactericidal activity against susceptible strains of staphylococci. While the combination regimens were bactericidal against this strain, due to the potent anti-staphylococcal activity of high-dose DAP against most susceptible strains, the magnitude of synergy with this combination may be smaller against other DAP-susceptible strains.

Conclusion. As DAP and VAN nonsusceptibility becomes more common in *S. aureus*, clinicians are left with fewer safe and effective treatment options for severe infections. The results of this study show that CPT given in conjunction with DAP is a potent combination against both DNS VISA and DAP-susceptible strains, resulting in rapid and sustained bactericidal activity. This combination is a promising option for the management of serious infections caused by MRSA with reduced susceptibility to VAN and DAP.

ACKNOWLEDGMENTS

This work was funded by an investigator-initiated grant from Forest Laboratories. Genome sequencing of the isolates was performed at STSI and funded by NIH/NCRR grant number UL1 RR025774. We thank Abbott Laboratories for the use of the fluorescence polarization immunoassay analyzer for determination of vancomycin concentrations.

M.J.R. has received grant support, consulted for, or provided lectures for Astellas, Cubist, Forest, Pfizer, Novartis, and Rib-X. M.J.R. is funded in part by NIH R21A1092055-01. G.S. has received grant support, consulted for, or provided lectures for Cubist, Astellas, Pfizer, and Ortho-McNeil Pharmaceuticals. W.E.R. has received grant support, consulted for, or provided lectures for Cubist, Astellas, and The Medicines Company. J.P. has received research grants and consulting fees from Cubist Pharmaceuticals. B.J.W. and R.T. have nothing to declare.

REFERENCES

1. **Boucher HW, Sakoulas G.** 2007. Perspectives on Daptomycin resistance, with emphasis on resistance in Staphylococcus aureus. Clin. Infect. Dis. **45**:601–608.
2. **Jones T, Yeaman MR, Sakoulas G, Yang SJ, Proctor RA, Sahl HG, Schrenzel J, Xiong YQ, Bayer AS.** 2008. Failures in clinical treatment of Staphylococcus aureus infection with daptomycin are associated with al-

terations in surface charge, membrane phospholipid asymmetry, and drug binding. Antimicrob. Agents Chemother. **52**:269–278.
3. **Liu C, Bayer A, Cosgrove SE, Daum RS, Fridkin SK, Gorwitz RJ, Kaplan SL, Karchmer AW, Levine DP, Murray BE, Rybak JM, Talan DA, Chambers HF.** 2011. Clinical practice guidelines by the Infectious Diseases Society of America for the treatment of methicillin-resistant Staphylococcus aureus infections in adults and children: executive summary. Clin. Infect. Dis. **52**:285–292.
4. **Villegas-Estrada A, Lee M, Hesek D, Vakulenko SB, Mobashery S.** 2008. Co-opting the cell wall in fighting methicillin-resistant Staphylococcus aureus: potent inhibition of PBP 2a by two anti-MRSA beta-lactam antibiotics. J. Am. Chem. Soc. **130**:9212–9213.
5. **Steed M, Vidaillac C, Rybak MJ.** 2011. Evaluation of ceftaroline activity versus daptomycin (DAP) against DAP-nonsusceptible methicillin-resistant Staphylococcus aureus strains in an in vitro pharmacokinetic/pharmacodynamic model. Antimicrob. Agents Chemother. **55**:3522–3526.
6. **Vidaillac C, Leonard SN, Rybak MJ.** 2009. In vitro activity of ceftaroline against methicillin-resistant Staphylococcus aureus and heterogeneous vancomycin-intermediate S. aureus in a hollow fiber model. Antimicrob. Agents Chemother. **53**:4712–4717.
7. **Mwangi MM, Wu SW, Zhou Y, Sieradzki K, de Lencastre H, Richardson P, Bruce D, Rubin E, Myers E, Siggia ED, Tomasz A.** 2007. Tracking the in vivo evolution of multidrug resistance in Staphylococcus aureus by whole-genome sequencing. Proc. Natl. Acad. Sci. U. S. A. **104**:9451–9456.
8. **Sieradzki K, Leski T, Dick J, Borio L, Tomasz A.** 2003. Evolution of a vancomycin-intermediate Staphylococcus aureus strain in vivo: multiple changes in the antibiotic resistance phenotypes of a single lineage of methicillin-resistant S. aureus under the impact of antibiotics administered for chemotherapy. J. Clin. Microbiol. **41**:1687–1693.
9. **Yang SJ, Xiong YQ, Boyle-Vavra S, Daum R, Jones T, Bayer AS.** 2010. Daptomycin-oxacillin combinations in treatment of experimental endocarditis caused by daptomycin-nonsusceptible strains of methicillin-resistant Staphylococcus aureus with evolving oxacillin susceptibility (the "seesaw effect"). Antimicrob. Agents Chemother. **54**:3161–3169.
10. **Finan JE, Archer GL, Pucci MJ, Climo MW.** 2001. Role of penicillin-binding protein 4 in expression of vancomycin resistance among clinical isolates of oxacillin-resistant Staphylococcus aureus. Antimicrob. Agents Chemother. **45**:3070–3075.
11. **Howden BP, Davies JK, Johnson PD, Stinear TP, Grayson ML.** 2010. Reduced vancomycin susceptibility in Staphylococcus aureus, including vancomycin-intermediate and heterogeneous vancomycin-intermediate strains: resistance mechanisms, laboratory detection, and clinical implications. Clin. Microbiol. Rev. **23**:99–139.
12. **Sieradzki K, Tomasz A.** 1999. Gradual alterations in cell wall structure and metabolism in vancomycin-resistant mutants of Staphylococcus aureus. J. Bacteriol. **181**:7566–7570.
13. **Yin S, Daum RS, Boyle-Vavra S.** 2006. VraSR two-component regulatory system and its role in induction of pbp2 and vraSR expression by cell wall antimicrobials in Staphylococcus aureus. Antimicrob. Agents Chemother. **50**:336–343.
14. **Dhand, A, Bayer. AS, Pogliano. J, Yang. SJ, Bolaris. M, Nizet. V, Wang. G, Sakoulas. G.** 2011. Use of antistaphylococcal {beta}-lactams to increase daptomycin activity in eradicating persistent bacteremia due to methicillin-resistant Staphylococcus aureus: role of enhanced daptomycin binding. Clin. Infect. Dis. **53**:158–163.
15. **Sakoulas G, Bayer AS, Pogliano J, Tsuji BT, Yang SJ, Mishra NN, Nizet V, Yeaman MR, Moise PA.** 2012. Ampicillin enhances daptomycin- and cationic host defense peptide-mediated killing of ampicillin- and vancomycin-resistant Enterococcus faecium. Antimicrob. Agents Chemother. **56**:838–844.
16. **Clinical and Laboratory Standards Institute.** 2012. Performance standards for antimicrobial susceptibility testing; 22nd informational supplement. CLSI, Wayne, PA.
17. **Riccobene T, Fang E, Thye D.** 2008. A single- and multiple-dose study to determine the safety, tolerability, and pharmacokinetics (PK) of ceftaroline (CPT) administered by intramuscular (IM) injection to healthy subjects, abstr A-1888. Abstr. 48th Annu. Intersci. Conf. Antimicrob. Agents Chemother. (ICAAC)-Infect. Dis. Soc. Am. (IDSA) 46th Annu. Meet. American Society for Microbiology and Infectious Diseases Society of America, 25–28 October 2008. Washington, DC.
18. **Benvenuto M, Benziger DP, Yankelev S, Vigliani G.** 2006. Pharmacokinetics and tolerability of daptomycin at doses up to 12 milligrams per kilogram of body weight once daily in healthy volunteers. Antimicrob. Agents Chemother. **50**:3245–3249.
19. **Leonard SN, Rybak MJ.** 2009. Evaluation of vancomycin and daptomycin against methicillin-resistant Staphylococcus aureus and heterogeneously vancomycin-intermediate S. aureus in an in vitro pharmacokinetic/pharmacodynamic model with simulated endocardial vegetations. J. Antimicrob. Chemother. **63**:155–160.
20. **Blaser J.** 1985. In-vitro model for simultaneous simulation of the serum kinetics of two drugs with different half-lives. J. Antimicrob. Chemother. **15**(Suppl. A):125–130.
21. **Kraus D, Herbert S, Kristian SA, Khosravi A, Nizet V, Gotz F, Peschel A.** 2008. The GraRS regulatory system controls Staphylococcus aureus susceptibility to antimicrobial host defenses. BMC Microbiol. **8**:85.
22. **Silverman JA, Perlmutter NG, Shapiro HM.** 2003. Correlation of daptomycin bactericidal activity and membrane depolarization in Staphylococcus aureus. Antimicrob. Agents Chemother. **47**:2538–2544.
23. **Pogliano J, Osborne N, Sharp MD, Abanes-De Mello A, Perez A, Sun YL, Pogliano K.** 1999. A vital stain for studying membrane dynamics in bacteria: a novel mechanism controlling septation during Bacillus subtilis sporulation. Mol. Microbiol. **31**:1149–1159.
24. **Kuroda M, Ohta T, Uchiyama I, Baba T, Yuzawa H, Kobayashi I, Cui L, Oguchi A, Aoki K, Nagai Y, Lian J, Ito T, Kanamori M, Matsumaru H, Maruyama A, Murakami H, Hosoyama A, Mizutani-Ui Y, Takahashi NK, Sawano T, Inoue R, Kaito C, Sekimizu K, Hirakawa H, Kuhara S, Goto S, Yabuzaki J, Kanehisa M, Yamashita A, Oshima K, Furuya K, Yoshino C, Shiba T, Hattori M, Ogasawara N, Hayashi H, Hiramatsu K.** 2001. Whole genome sequencing of meticillin-resistant Staphylococcus aureus. Lancet **357**:1225–1240.
25. **Li H, Durbin R.** 2009. Fast and accurate short read alignment with Burrows-Wheeler transform. Bioinformatics **25**:1754–1760.
26. **Lunter G, Goodson M.** 2011. Stampy: a statistical algorithm for sensitive and fast mapping of Illumina sequence reads. Genome Res. **21**:936–939.
27. **DePristo MA, Banks E, Poplin R, Garimella KV, Maguire JR, Hartl C, Philippakis AA, del Angel G, Rivas MA, Hanna M, McKenna A, Fennell TJ, Kernytsky AM, Sivachenko AY, Cibulskis K, Gabriel SB, Altshuler D, Daly MJ.** 2011. A framework for variation discovery and genotyping using next-generation DNA sequencing data. Nat. Genet. **43**:491–498.
28. **Hernandez D, Francois P, Farinelli L, Osteras M, Schrenzel J.** 2008. De novo bacterial genome sequencing: millions of very short reads assembled on a desktop computer. Genome Res. **18**:802–809.
29. **Cui L, Ma X, Sato K, Okuma K, Tenover FC, Mamizuka EM, Gemmell CG, Kim MN, Ploy MC, El-Solh N, Ferraz V, Hiramatsu K.** 2003. Cell wall thickening is a common feature of vancomycin resistance in Staphylococcus aureus. J. Clin. Microbiol. **41**:5–14.
30. **Wootton M, Howe RA, Hillman R, Walsh TR, Bennett PM, MacGowan AP.** 2001. A modified population analysis profile (PAP) method to detect hetero-resistance to vancomycin in Staphylococcus aureus in a UK hospital. J. Antimicrob. Chemother. **47**:399–403.
31. **Peschel A, Jack RW, Otto M, Collins LV, Staubitz P, Nicholson G, Kalbacher H, Nieuwenhuizen WF, Jung G, Tarkowski A, van Kessel KP, van Strijp JA.** 2001. Staphylococcus aureus resistance to human defensins and evasion of neutrophil killing via the novel virulence factor MprF is based on modification of membrane lipids with L-lysine. J. Exp. Med. **193**:1067–1076.
32. **Rose WE, Schulz LT, Andes D, Striker R, Berti AD, Hutson PR, Shukla SK.** 2012. Addition of ceftaroline to daptomycin after the emergence of daptomycin-nonsusceptible Staphylococcus aureus during therapy improves anti-bacterial activity. Antimicrob. Agents Chemother. **56**:5296–5302.
33. **Sakoulas G, Rose WE.** 2011. Effect of beta-lactam (BL) exposure in vitro on daptomycin (DAP) activity and cell wall thickness in MRSA, poster E-1332. Abstr. 51st Annu. Intersci. Conf. Antimicrob. Agents Chemother., Chicago, IL.
34. **Steed ME, Vidaillac C, Rybak MJ.** 2010. Novel daptomycin combinations against daptomycin-nonsusceptible methicillin-resistant Staphylococcus aureus in an in vitro model of simulated endocardial vegetations. Antimicrob. Agents Chemother. **54**:5187–5192.
35. **Steed ME, Werth BJ, Ireland CE, Rybak MJ.** 2012. Evaluation of the novel combination of high-dose daptomycin plus trimethoprim-sulfamethoxazole against daptomycin nn-susceptible methicillin-resistant Staphylococcus aureus using an in vitro pharmacokinetic/

pharmacodynamic model of simulated endocardial vegetations. Antimicrob. Agents Chemother. **56**:5709–5714.
36. **Hagihara M, Wiskirchen DE, Kuti JL, Nicolau DP.** 2012. In vitro pharmacodynamics of vancomycin and cefazolin alone and in combination against methicillin-resistant Staphylococcus aureus. Antimicrob. Agents Chemother. **56**:202–207.
37. **Leonard SN.** 2012. Synergy between vancomycin and nafcillin against Staphylococcus aureus in an in vitro pharmacokinetic/pharmacodynamic model. PLoS One **7**:e42103. doi:10.1371/journal.pone.0042103.
38. **Berti AD, Wergin JE, Girdaukas GG, Hetzel SJ, Sakoulas G, Rose WE.** 2012. Altering the proclivity towards daptomycin resistance in methicillin-resistant Staphylococcus aureus using combination with other antibiotics. Antimicrob. Agents Chemother. **56**:5046–5053.
39. **Yang SJ, Nast CC, Mishra NN, Yeaman MR, Fey PD, Bayer AS.** 2010. Cell wall thickening is not a universal accompaniment of the daptomycin nonsusceptibility phenotype in Staphylococcus aureus: evidence for multiple resistance mechanisms. Antimicrob. Agents Chemother. **54**:3079–3085.
40. **Xiong YQ, Mukhopadhyay K, Yeaman MR, Adler-Moore J, Bayer AS.** 2005. Functional interrelationships between cell membrane and cell wall in antimicrobial peptide-mediated killing of Staphylococcus aureus. Antimicrob. Agents Chemother. **49**:3114–3121.

AAC
Journals.ASM.org

ERRATUM

Ceftaroline Increases Membrane Binding and Enhances the Activity of Daptomycin against Daptomycin-Nonsusceptible Vancomycin-Intermediate *Staphylococcus aureus* in a Pharmacokinetic/Pharmacodynamic Model

Brian J. Werth, George Sakoulas, Warren E. Rose, Joseph Pogliano, Ryan Tewhey, Michael J. Rybak

Anti-Infective Research Laboratory, Department of Pharmacy Practice, Eugene Applebaum College of Pharmacy and Health Sciences, and Department of Internal Medicine, Division of Infectious Diseases, School of Medicine, Wayne State University, Detroit, Michigan, USA; Department of Medicine, New York Medical College, Valhalla, New York, USA; University of California San Diego School of Medicine, La Jolla, California, USA; University of California San Diego Division of Biology, La Jolla, California, USA; School of Pharmacy, University of Wisconsin—Madison, Madison, Wisconsin, USA; and Scripps Translational Science Institute, Scripps Research Institute, La Jolla, California, USA

Volume 57, no. 1, p. 66–73, 2013. Page 66: Abstract, line 4, "Simulations of ceftaroline-fosamil at 600 mg per kg of body weight every 8 h (q8h). . ." should read "Simulations of ceftaroline-fosamil at 600 mg every 8 h (q8h). . ."

doi:10.1128/AAC.00069-13